Hadron Helicity Violation in Exclusive Processes: Quantitative Calculations in Leading Order QCD

Thierry Gousset

CEA, Service de Physique Nucléaire/DAPNIA,
CE Saclay, F91191 Gif, France
and
Centre de Physique Théorique,
Ecole Polytechnique, F91128 Palaiseau, France

Bernard Pire

Centre de Physique Théorique,
Ecole Polytechnique, F91128 Palaiseau, France

John P. Ralston

Department of Physics and Astronomy
and
Kansas Institute for Theoretical and Computational Science,
University of Kansas, Lawrence, Kansas 66045 USA

Abstract

We study a new mechanism for hadronic helicity flip in high energy hard exclusive reactions. The mechanism proceeds in the limit of perfect chiral symmetry, namely without any need to flip a quark helicity. The fundamental feature of the new mechanism is the breaking of rotational symmetry of the hard collision by a scattering plane in processes involving independent quark scattering. We show that in the impulse approximation there is no evidence for of the helicity violating process as the energy or momentum transfer Q^2 is increased over the region $1\,GeV^2 < Q^2 < 100\,GeV^2$. In the asymptotic region $Q^2 > 1000$ GeV^2, a saddle point approximation with doubly logarithmic accuracy yields suppression by a fraction of power of Q^2. "Chirally–odd" exclusive wave functions which carry non–zero orbital angular momentum and yet are leading order in the high energy limit, play an important role.

1 Introduction

The theory of hard elastic scattering in Quantum Chromodynamics (QCD) has evolved considerably over many years of work. Currently there exist two self-consistent perturbative descriptions, each with a specific factorization method for separating the hard scattering from non-perturbative wave functions. A well-known procedure using the "quark-counting" diagrams has been given by Lepage and Brodsky [1]. A consequence, and direct test, of the factorization defining this mechanism is the hadron helicity conservation rule [2]

$$\lambda_A + \lambda_B = \lambda_C + \lambda_D \ , \tag{1}$$

where the λ_j's are the helicities of the participating hadrons in the reaction $A + B \to C + D$. The fact that this rule is badly violated in almost every case tested suggests two alternatives. One possibility, advocated by Isgur and Llewellyn-Smith [3], is that the energy and momentum transfer (Q^2) in the data is not large enough for the formalism to apply. However, the data also shows behavior close to the model's predicted power dependence on Q^2, indicating that hard scattering of a few pointlike quarks is being observed. The apparent contradiction has led to much discussion, and has even caused some authors to suggest that perturbative QCD itself might be wrong.

The second alternative is that another power behaved process causing helicity flip is present. In fact the "independent scattering" subprocess, introduced by Landshoff [4], is actually the leading process at very high energies [5]. But it has been assumed that hadron helicity conservation would be the same in the independent scattering process as in the quark-counting one, since both involve exchange of hard gluons with large Q^2. In general, terms proportional to a quark mass, m_q, for example, have been understood to cause helicity flip in either model, but with amplitude suppressed by a power of m_q/Q relative to the leading term. Such terms seem to be quite small and are probably not a believable explanation of the persistent pattern of large violations of the helicity conservation rule.

Here we show that the independent scattering mechanism predicts high-energy helicity *non-conservation* at a much higher rate. The calculations in momentum space are sufficiently complicated that this phenomenon has been overlooked for almost twenty years. Adopting a transverse position space formalism introduced by Botts and Sterman [6], we show that the details rest on non-perturbative wave functions that should be *measured* rather than calculated. These wave functions measure non–zero orbital angular momentum not taken into account by short distance expansions. We argue that the novel factorization properties of independent scattering processes cannot practically be reduced to the same ingredients used in the quark counting scattering. In any case, it is not necessary to flip a quark helicity: the new mechanism proceeds unimpeded in the limit of arbitrarily small quark mass and perfect chiral symmetry in the hard scattering.

This paper is organized as follows. In section 2 we review the derivation of helicity conservation in genuine short distance processes.. In section 3, we present the independent scattering mechanism with special emphasis on non-zero orbital angular momentum wave functions. We compute the contribution of these components to a helicity conserving reaction in section 4, then to a helicity violating reaction in section 5. These two sections contain our most important results at asymptotic and at accessible energies. Section 6 is an experimental outlook.

2 Helicity conservation in short distance dominated processes

First we review the conventional derivation of hadron helicity conservation [2]. The quark-counting factorization introduces the distribution amplitude $\varphi(Q^2, x)$ [7], an integral over the transverse momentum variables of the wave function for quarks to be found carrying momentum fraction x in the hadron.[1] For simplicity of presentation we specialize to a single pair of quarks, the meson case. Let $\psi(\mathbf{k}_T, x)$ be a light cone wave function to find quarks with relative transverse momentum $\mathbf{k}_T$ and light cone momentum fraction x. In terms of the Fourier conjugate transverse space variable $\mathbf{b}_T$ separating the quarks, then

$$\begin{aligned}\varphi(Q^2, x) &= \int_0^Q d^2\mathbf{k}_T\ \psi(\mathbf{k}_T, x) \\ &= \int_0^Q d^2\mathbf{k}_T \int_0^\infty d^2\mathbf{b}_T e^{i\mathbf{b}_T\cdot\mathbf{k}_T} \sum_m e^{im\varphi}\tilde{\psi}_m(\mid \mathbf{b}_T \mid, x)\end{aligned} \tag{2}$$

In the second line we have expanded the wave function $\tilde{\psi}(\mathbf{b}_T, x)$ to exhibit the $SO(2)$ orbital angular momentum eigenvalues m: a complete set for the (nearly on-shell) quarks consists of the z-axis orbital angular momentum, the energy, and the z-momentum. Now suppose the distribution amplitude $\varphi(Q^2, x)$ is assumed to be a good description of a process. Then, whatever the angular momentum of the wave function, evaluating the integrals reveals the $m = 0$ element is the sole surviving term in Eq. (2):

$$\varphi(Q^2, x) = 2\pi \int_0^\infty d \mid \mathbf{b}_T \mid Q J_1(\mid \mathbf{b}_T \mid Q)\tilde{\psi}_0(\mid \mathbf{b}_T \mid, x) \tag{3}$$

This shows that use of $\varphi(Q^2, x)$ imposes two things: as $Q^2 \to \infty$ the scattering region is both "small", since the region $\mathbf{b}_T^2 < 1/Q^2$ dominates in the Bessel function, and the scattering is "round", *i.e.* cylindrically symmetric (Fig. 1). In the absence of orbital angular momentum, the hadron helicity becomes the sum of the quark helicities. The quark helicities being conserved at leading order, the total hadron helicities are conserved. The hadron helicity conservation rule (1) therefore represents an exact *symmetry* of the quark-counting factorization. A crucial question is: does this symmetry of the model represent a property of the entire perturbative theory. Or, can we simply assume "s–wave" $SO(2)$ wave functions to be the main contribution as in a non–relativistic picture?

The answer to both questions is *no*. In general, quark wave functions themselves are not particularly restricted in orbital angular momentum content, even in the high energy limit. For example, in the pion (pseudoscalar meson) case the light-cone wave function may be expanded on four Dirac tensors allowed by parity symmetry as

$$\tilde{\psi}_{\alpha\beta}(x, \mathbf{b}_T; p^\mu) = \{A_\pi \not{p}\gamma_5 + B_\pi\gamma_5 + C_\pi \not{b}_T\gamma_5 + D_\pi[\not{p}, \not{b}_T]\gamma_5\}_{\alpha\beta}\,, \tag{4}$$

[1] Our convention does not include a logarithmically varying factor of Q^2 introduced for renormalization group analysis in Ref. [1, 7]. Either convention can be used without affecting our argument.

where A_π-D_π are functions of the light cone fraction x, the transverse separation $\mathbf{b}_T$ and the total four momentum of the meson p^μ. For the moment we do not discuss dependence on gauge fixing and a path-ordered exponential of the gauge potential used to make the wave function gauge invariant. The D_π-term carries one unit of orbital angular momentum and yet scales with the same power of the "big" momentum p^+ as the A_π–term, which is s-wave. Since the D_π term has a $\vec{b}_T$ factor, which can be written in terms of $b_{T,1} \pm i b_{T,2}$ this term represents one unit of orbital angular mometum. In terms of power counting, then, the $m = 0$ and $m \neq 0$ amplitudes can be equally large. We also note that wave functions are not objects to be derived in perturbation theory, but instead represent the long-time, non-perturbative time evolution proceeding inside a hadron. The non-perturbative Hamiltonian of QCD does not conserve spin and orbital angular momentum separately, but instead generates mixing between orbital and spin angular momentum. Finally, there is no simple relation between "s–wave" non–relativistic models of constituent quarks, and the pointlike quarks resolved in large–Q^2 collisions, so no statement can reliably be made about quark angular momentum content of hadrons. Thus *if* a non-zero orbital angular momentum component somehow enters the hard scattering — and this is a crucial point — *then* the long-time evolution before or after the scattering can convert this angular momentum into the observed hadron spin. It is not necessary to flip a quark spin in the hard interaction, because the asymptotic hadron spin fails to equal the sum of the quark spins. Such a mechanism is totally consistent with the impulse approximation of perturbative QCD.

The challenge in high energy hadron scattering is therefore to find those large Q^2 process(es) in which non-zero orbital angular momentum enters, or in other words, to find those which are not "round". It turns out that in any treatment relevant to current energies the independent scattering process is not "round" but instead "flat" (Fig. 1). The subprocess is highly asymmetric, showing an extreme dependence on the scattering plane. Rather than disappearing in the high energy limit, the dynamics of this process *increases its asymmetry over a range of* Q^2.

The origin of the asymmetry is kinematic. Let η be the direction perpendicular to the scattering plane and ξ be a vector in the scattering plane. In the independent scattering mechanism, let two (or more) uncorrelated scattering planes be separated at the collision point by a transverse out–of–plane distance b_η. The out–going beams of quarks must coincide in direction well enough to make hadrons in the final state. Conserving 4-momenta, for each pair of scatterings there are three delta functions of large momenta (scaling like p^+), and one delta function of the out-of plane transverse momentum, of the order of $1/ < b_\eta^2 >^{1/2}$, where $<>$ indicates a typical expectation value in the state. On–shell quark–quark scattering is dimensionless and scale invariant (up to logarithmic corrections) in QCD. The overall amplitude therefore scales like the product of these factors, namely like $< b_\eta^2 >^{1/2} (Q^2)^{-3/2}$. The Q^2 power-counting of this argument is quite well-known; what we emphasise here is the role of the scattering plane, namely the breaking of rotational symmetry with the out-of-plane direction η. It is as if hadrons "flatten" under impact in the in-plane direction ξ, forming a cigar-shaped hard scattering region [9]. This fact is very hard to see in covariant perturbation theory in momentum space, explaining why it has generally been overlooked.

The kinematic violation of hadron helicity conservation by independent scattering raises several new questions. It is clear that the usual association of leading–twist (short–distance)

and large Q^2 either breaks down or hinges on delicate dynamical details. Our approach will exploit the fact that leading approximations to any kinematically distinct amplitude are always perturbatively calculable. For example, higher order corrections of non–leading twist type in the distibution amplitude formalism cannot violate the hadron helicity conservation symmetry and will not affect our approach. The first non–vanishing contributions to helicity violating amplitudes involve extra partons in the short distance formalism. A gluon embedded in the hard scattering, for example, could transfer spin to an outgoing hadron. We need not consider such processes, because, as discussed later, they are subleading by a power of Q^2 and perturbatively small since such gluons are "hard". It remains to be shown, of course, that helicity violation from independent scattering is not suppressed by the same order. That is the main technical task of this paper.

3 Independent scattering: formalism

3.1 Kinematical analysis

Botts and Sterman have considered [6] the generic "elastic" reaction $M_1 + M_2 \to M_3 + M_4$, where M_i's are light pseudoscalar mesons, at high energy $\sqrt{s}$ and large angle center of mass scattering angle $\theta = \arccos(1 + 2t/s)$. Their study has shown that the reaction is dominated by the 2 independent scatterings of the valence constituents with a kinematical configuration depicted in Fig. 2. One has two scattering planes separated at the collision point by a transverse distance b.

To make it clear, let us consider a light cone basis (v_i, v_i', ξ_i, η) attached to each meson M_i, and chosen so that, in the center of mass frame where $\widehat{p_1} = \hat{3}$ and $\widehat{p_3} = \cos\theta\,\hat{3} + \sin\theta\,\hat{1}$,

$$
\begin{aligned}
&v_1 = v_2' = \tfrac{1}{\sqrt{2}}(\hat{0} + \hat{3}); && v_1' = v_2 = \tfrac{1}{\sqrt{2}}(\hat{0} - \hat{3});\\
&\xi_1 = \xi_2 = \hat{1}; && \eta = \hat{2};\\
&v_3 = v_4' = \tfrac{1}{\sqrt{2}}(\hat{0} + \sin\theta\,\hat{1} + \cos\theta\,\hat{3}); && v_3' = v_4 = \tfrac{1}{\sqrt{2}}(\hat{0} - \sin\theta\,\hat{1} - \cos\theta\,\hat{3});\\
&\xi_3 = \xi_4 = \cos\theta\,\hat{1} - \sin\theta\,\hat{3}.
\end{aligned}
$$

In the cm frame, one has $p_i = Qv_i$ ($Q = \sqrt{s/2}$). Each Bethe-Salpeter amplitude X_i

$$X_i(k, p_i) = \int \frac{d^4k}{(2\pi)^4} e^{ik.y} \langle 0|T(\psi_\alpha(y)\bar{\psi}_\beta(0))|\pi(p_i)\rangle,$$

is assumed to eliminate $q\bar{q}$ configuration with relative $O(Q)$ transverse momentum (along ξ_i and η). The relative minus momentum (along v_i') is of $O(M^2/Q)$. Then, momentum transfers in H or H' are dominated by large invariants built with x_iQ-terms and a first approximation is to neglect all but these components of the quark or antiquark momenta, in the hard amplitudes H and H'. This is the impulse approximation.

A second observation follows from kinematics; although momentum conservation at the hard scattering H relates the internal momentum dependence of the X's, a variation of one such momentum k_i in its ξ_i or v_i' direction induces negligible modifications in the three other

X's. Consequently, momentum components of k_i along ξ_i or v_i' only appear as a relevant variable in the wave function X_i and integrals over these components can be carried out. The components along η, denoted l_i, represent transverse momentum out of the scattering plane and do not share the same property. Thus, the vertex delta function may be reexpressed as

$$\delta^4(k_1+k_2-k_3-k_4)=\frac{\sqrt{2}}{|\sin\theta|Q^3}\prod_{i=2}^{4}\delta(x_1-x_i)\,\delta(l_1+l_2-l_3-l_4),$$

which indicates that the 4 constituents which enter or leave each hard scattering carry the same light cone fraction ($x_i = x$ or $1-x$). Introducing the "out of plane" impact parameter b through

$$2\pi\delta(l_i)=\int_{-\infty}^{+\infty}db\,e^{i(l_1+l_2-l_3-l_4).b},$$

one may write the amplitude of the process [6] as

$$A(s,t)=\frac{\sqrt{2}Q}{2\pi|\sin\theta|}\int_0^1 dx\,(2\pi)^4 H(\{xQv\})\,H'(\{\bar{x}Qv\})\Big|_{\{\alpha,\beta\}}\int_{-\infty}^{+\infty}db\prod_{i=1}^{4}\mathcal{P}_{\alpha_i\beta_i}(x,b,Qv_i). \quad (5)$$

where $\mathcal{P}$ is the amplitude

$$\mathcal{P}_{\alpha\beta}(x,b,Qv)=\int\frac{dy^-}{2\pi}\,e^{ixQy^-}<0|\,T\,(q_\alpha(y)\,\bar{q}_\beta(0))\,|\pi(Qv)>\Big|_{y=y^-v'+b\eta}, \quad (6)$$

with Dirac indices $\alpha\beta$. Color indices are suppressed in Eq. (5) and sums over repeated indices are understood. We consider unflavored quarks. The implementation of flavor is straightforward by setting to 0 some of the graphs we are going to consider. H and H' are Feynman amplitudes (a sum over allowed diagrams is understood) at the level of quarks computed with standard perturbative QCD vertices and internal propagators; they consist, at lowest order in the coupling constant, of one-gluon exchange or $q\bar{q}$ annihilation for each quark pair. Note that $\mathcal{P}$ and H are not individually gauge invariant. If the short–distance $b\to 0$ limit is assumed, then the four general wave functions in Eq. (4) can be reduced to one A_π–term, by taking the trace $\mathcal{P}_0$ of $\mathcal{P}_{\alpha\beta}$ with $Q\not{v}'\gamma^5_{\alpha\beta}$. For the case of helicity conserving amplitudes, this selection was shown to be self–consistent by Botts and Sterman[6]. Then, the zeroth moment of $\mathcal{P}_0$ is related to the decay constant of the corresponding meson

$$\int_0^1 dx\mathcal{P}_0(x,b=0,p=Qv)=f_M$$

where, *e.g.* for the pion, $f_\pi = 133MeV$. This zero–distance quantity contains no information on the interesting dependence on the transverse variable b.

Here we are concerned with the leading order description of helicity violating terms. Thus, we will consider A_π–type and D_π–type amplitudes on an equal footing, and make no a priori assumption that the region $b\to 0$ dominates.

3.2 Gauge Invariance

The development so far has been sufficient to isolate the kinematic region of interest, which as we have already noted is characterized by finite separation between the participating quarks

in the out-of scattering plane direction. The amplitude is thus a strong function of the spatial dependence of the wave function. The Bethe Salpeter wave function is a bilocal matrix element and is not gauge invariant. However, we will now discuss how gauge invariance of the description can be obtained.

The key is in how the perturbation theory is re-arranged. In the Sterman and Botts factorization certain "soft" corrections are put into the wave functions, leaving other parts of Feynman diagrams to go into the hard scattering kernel. In dressing the wave function in this way, it is no longer a quark correlation (the Bethe Salpeter wave function), but the matrix elements of operators determined by the types of diagrams put in. The operators chosen in [6] are path ordered exponentials (poe's), shown by Collins and Soper [8] to be the generators of eikonal approximations to the gluon attachments. The poe's are gauge covariant, leading to a gauge invariant amplitude.

This is partly forced by physics, and partly a convention. As a convention for the perturbation theory, subsequent diagrams must be evaluated with subtractions to avoid double-counting. More generally, any operator functional of the A fields which transforms properly could serve in place of the poe's, and creating a different subtraction procedure. Let us extract what we can that is independent of convention.

Let the operator in the definition of the wave functions be called $U(A;x)$; we will call it a gauge-dressing operator. Under a gauge transformation at the position x, we require $U(A;x)$ to transform like an antiquark. Then products such as $U(A;x)\,\psi(x)$ are gauge invariant. That is, we have gauge invariant matrix elements to find a dressed quark

$$\langle 0|T(U(A;y)\psi(y)\,U^\dagger(A;x)\bar\psi(x))|\pi(p)\rangle$$

It is obvious that this requirement does not determine $U(A;x)$ uniquely, because one could always attach a factor which is gauge invariant without changing the gauge transformation properties. The particular choice of what to attach is a prescription, *i.e.* a definition of what parts of the amplitude will be put in the wave function and what in the hard scattering, and it cannot be determined by gauge invariance alone. However, due to gauge transformations one must attach some kind of gauge-dressing operator to have a well defined matrix elements.

3.3 Path-Independent Dressing

Although the standard way to do gauge dressing with the poe is path dependent, no path dependence generally need be associated with $U(A;x)$ and in particular the observable process does not determine or favor any path. This important point can be seen with an elementary example from QED, where the $U(1)$ gauge invariance is easier to control. The straightforward QED analogue of our process involves equal time (not light cone time) correlation functions in the gauge $A^0 = 0$. This gauge choice eliminates a mode, but there still remains a lack of definition of the coordinates due to time independent gauge transformations $\theta(x)$

$$\mathbf{A}(x) \to \mathbf{A}'(x) = \mathbf{A}(x) + \nabla\theta(x),\ \partial^0\theta = 0$$

This produces a change in the longitudinal modes. These modes are sometimes also called unphysical, a very unfortunate choice of terminology. In free space and in the absence of coupling a gauge theory has two transverse degrees of freedom and the third would be called

unphysical. However we are interested in the case that matter fields exist (and the non-Abelian coupling is turned on) in which case the third mode is real, but special inasmuch as being constrained in terms of the other variables by gauge invariance. To see this, note that we can decompose into transverse and longitudinal parts,

$$\begin{aligned} \mathbf{A} &= \mathbf{A}_T + \mathbf{A}_L \\ &= \mathbf{A}_T + \nabla\phi \\ \phi &= \left[\frac{1}{\nabla^2}\nabla\cdot\mathbf{A}\right](x) \qquad \text{(transforming part)} \\ \mathbf{A}_T &= \mathbf{A} - \nabla\phi \qquad\qquad \text{(invariant part).} \end{aligned} \tag{7}$$

Since it is there for gauge transformations, the longitudinal part ϕ is not free to be varied in arbitrary dynamical ways, but must accompany the matter field in a prescribed, unique functional. At time $t = 0$ this operator is

$$U(A;x) = e^{ig\phi(x)} \tag{8}$$

from which one can verify that under a gauge transformation,

$$\begin{aligned} \phi(x) &\rightarrow \phi(x) + \theta(x) \\ \psi(x) &\rightarrow e^{-ig\theta(x)}\psi(x) \\ U(A;x) &\rightarrow e^{ig\theta(x)}U(A;x) \\ U(A;x)\psi(x) &\rightarrow U(A;x)\psi(x) \end{aligned} \tag{9}$$

We will call this the Coulomb dressing because it creates a classical Coulomb field around the matter particle, as the reader can check by calculation. Since the Hamiltonian commutes with the gauge transformation operator once $A^0 = 0$ has been set, the time evolution will maintain the invariance of the combination $U(A;x)\psi(x)$. However, as noted already, one is not forced to accept this as the unique answer, but can opt for $U(A;x)\,f(\mathbf{A}_T)$, which will transform in the same way for any $f(\mathbf{A}_T)$.

The reader may still be curious to know the relation between Coulomb dressing and the poe approach. This can be very simply exhibited by noting that

$$\psi(y)e^{ig\phi(y)}e^{-ig\phi(x)}\bar{\psi}(x) = \psi(y)e^{ig\int_x^y d\mathbf{z}.\nabla(\phi)(\mathbf{z})}\bar{\psi}(x) \tag{10}$$

This expression is still path independent. This is the choice $f(\mathbf{A}_T) = 1$. A different choice is

$$f(\mathbf{A}_T) = e^{ig\int_x^y d\mathbf{z}.\mathbf{A}_T(\mathbf{z})} \tag{11}$$

in which case we have

$$U(A;y)U^\dagger(A;x)f(\mathbf{A}_T) = e^{ig\int_x^y d\mathbf{z}.\mathbf{A}(\mathbf{z})} \tag{12}$$

which is the standard path dependent poe. Both procedures are equally acceptable, as far as satisfying gauge invariance, but the path ordered exponential can create a line of physical transverse gauge field particles between the charged matter fields, depending on how it is oriented. Such a line of gluons, existing only along the chosen part, can be interpreted as

an arbitrary model for the transverse gauge field inside the state of interest. Similarly, if one boosts the Coulomb dressed definition, the boost also creates a blast of transverse gauge fields as seen by the "equivalent photon" approximation.

In perturbation theory, the lowest order approximation to non-Abelian dressing is the Abelian case. It is possible in the non-Abelian theory to write down expressions analogous to the Coulomb dressing but care must be used to keep track of the color indices. It is equally valid to use poe's, which definitely transform properly, as building blocks to generate an infinite number of different ways to dress the quarks. The different choices are not relevant for a leading order calculation to which we restrict this study.

3.4 Factorization

The next crucial step is to elaborate a factorized form for the amplitude, whose prototype is Eq. (5), regarding radiative corrections. Generalizing the results of [6] to the case of the helicity–violating Dirac projections, a leading approximation to the soft region rearranges these corrections to obtain the following expression

$$A(s,t) = \frac{\sqrt{2}Q}{2\pi|\sin\theta|}\int_0^1 dx\, H(\{xQv\})\, H'(\{\bar{x}Qv\}) \int_{-1/\Lambda}^{+1/\Lambda} db\, U(x,b,Q)\left(\mathcal{P}^{(0)}(x,b;1/|b|)\right)^4, \quad (13)$$

where H and H' are evaluated at respective scales xQ and $\bar{x}Q$ which are assumed to be large. Large logarithmic corrections to the process, with the coexistence of the two scales Q and $1/b$, are resummed in U, in such a way that $\mathcal{P}^{(0)}$ is now a soft object: it does not include perturbative corrections harder than $1/b$. It is the non perturbative object necessary to connect short and long range physics, both present in hard hadronic processes.

Expressions for the above quantities will be given in the phenomenological study, but let us specify here some of their qualitative features. When b is small, smaller or of the order of $1/Q$, radiative corrections are also small and must be considered as perturbative corrections to the hard amplitudes H or H'; in this regime, $\mathcal{P}^{(0)}$ is closely related to the distribution amplitude $\varphi(x;\mu)$ evaluated at the renormalization scale $\mu = 1/b$ [6]. Depending on the definition, the distribution amplitude also includes resummed logarithmic corrections from hadronic scale up to μ [1, 7]. When b is large, this replacement is not legitimate but since $U(b)$ is a strong suppression factor in this region the exact value of $\mathcal{P}^{(0)}$ is irrelevant.

Endpoints in the x integral where hard subprocesses would indeed become soft may look problematic. Both the distribution amplitude and wave function approaches used here become self–consistent because of the end–point zeroes, e.g. $\varphi(x \to 0) \sim x^k$, where $k > 0$ which should occur independently of spin projection.

4 Contribution from non-zero orbital momentum components of the wave function: $\pi\pi \to \pi\pi$

Before analyzing helicity violating processes let us examine the leading contribution from the various components in Eq. (4) to a standard helicity conserving reaction such as $\pi\pi \to \pi\pi$.

4.1 Computation of hard amplitudes

In their study, Botts and Sterman were interested in identifying the asymptotic behavior of the amplitude $A(s,t)$ ($s \to +\infty, \frac{t}{s}$ fixed). Asymptotically, the Sudakov mechanism contained in $U(b)$ results in a suppression of large b region in the integral of Eq. (13). In this limit one can forget about tensorial components of $\mathcal{P}_{\alpha\beta}(x,b,Qv) \propto (\cdots \not{b} \cdots)_{\alpha\beta}$ and only the projection of $P_{\alpha\beta}(x,b,Qv)$ onto the particular tensor $\frac{1}{4}\gamma_5 \not{v}|_{\alpha\beta}$ survives.

In the intermediate Q^2 regime, configurations of the $q\bar{q}$ pair sitting in a light meson with transverse separation smaller than the meson charge radius are not strongly affected by the Sudakov mechanism [10]. As anticipated in section 2, $m = 1$ components of the wave function which form large invariants in H (as large as the s-wave term) may give sizeable corrections to the interaction amplitude between pure s-wave states. For contributions with leading power behavior in the pseudoscalar case, we must keep the tensorial decomposition

$$\mathcal{P}_{\alpha\beta}(x,b,Qv) = \frac{1}{4}\gamma_5 \left\{ \mathcal{P}_0(x,b,Qv) \not{v} + \mathcal{P}_1(x,b,Qv) [\not{v}, \not{b}] \right\}_{\alpha\beta} . \tag{14}$$

We now explore the calculation with this assumption. To begin with, one forms the projection, denoted as t and t', of the hard amplitudes H and H' on the relevant various Dirac tensors coming from the wavefunction decomposition. We follow Botts and Sterman's classification of graphs, with three fermionic flows for H and two gluonic channels each (see Fig. 3),

f	$H(M_1M_2 \to M_3M_4)$	gluon	$c^f_{1,\{a_i\}}$	$c^f_{2,\{a_i\}}$
1	$1\bar{2} \to \bar{3}4$	$u,\ s$	$\delta_{a_1a_2}\delta_{a_3a_4}$	$\delta_{a_1a_4}\delta_{a_2a_3}$
2	$1\bar{2} \to 3\bar{4}$	$t,\ s$	$\delta_{a_1a_2}\delta_{a_3a_4}$	$\delta_{a_1a_3}\delta_{a_2a_4}$
3	$12 \to 34$	$t,\ u$	$\delta_{a_1a_4}\delta_{a_2a_3}$	$\delta_{a_1a_3}\delta_{a_2a_4}$

Color flow in this problem is simplified by noting that one gluon exchange between two quark lines gives a color tensor

$$\sum_c T^c_{ij} T^c_{kl} = \frac{1}{2}\left(\delta_{il}\delta_{kj} - \frac{1}{3}\delta_{ij}\delta_{kl} \right),$$

which we may reexpress with the color tensors listed above, in the form

$$[t \text{ or } u1]_{\{a_i\}} = \sum_{I=1}^{2} C_I c^f_{I\{a_i\}},\ [s \text{ or } u3]_{\{a_i\}} = \sum_{I=1}^{2} \tilde{C}_I c^f_{I\{a_i\}},$$

with

$$C_1 = \tilde{C}_2 = \frac{1}{2},\ C_2 = \tilde{C}_1 = -\frac{1}{6}.$$

With this notation, one finds for the hard amplitude a_0, containing no b factor,

$$\begin{aligned}
(t_I t_J)^{(1)}_0 &= C_I C_J \frac{s^2+t^2}{u^2} + (\tilde{C}_I C_J + C_I \tilde{C}_J)\frac{t^2}{su} + \tilde{C}_I \tilde{C}_J \frac{t^2+u^2}{s^2}; \\
(t_I t_J)^{(2)}_0 &= C_I C_J \frac{s^2+u^2}{t^2} + (\tilde{C}_I C_J + C_I \tilde{C}_J)\frac{u^2}{st} + \tilde{C}_I \tilde{C}_J \frac{t^2+u^2}{s^2}; \\
(t_I t_J)^{(3)}_0 &= C_I C_J \frac{s^2+u^2}{t^2} + (\tilde{C}_I C_J + C_I \tilde{C}_J)\frac{s^2}{tu} + \tilde{C}_I \tilde{C}_J \frac{s^2+t^2}{u^2};
\end{aligned} \tag{15}$$

times an overall common factor

$$\left(\frac{\pi}{6}\right)^4 \frac{32g^4}{x^2\bar{x}^2s^2},$$

where g is the QCD coupling constant which appears in Feynman rules. We have already indicated that the whole amplitude Eq. (13) can be properly defined regarding renormalization and factorization, so that g^4 stands for $(4\pi)^2\alpha_S(xQ)\alpha_S(\bar{x}Q)$.

There is no b^1 or b^3 terms, due to the odd number of γ matrices; this is a consequence of chiral symmetry. The second term is therefore a hard amplitude a_2, containing b^2, which is found to be

$$\begin{aligned}
(t_It_J)_2^{(1)} &= C_IC_J\frac{2st}{u^2} + (\tilde{C}_IC_J + C_I\tilde{C}_J)\frac{su-t^2}{su} + \tilde{C}_I\tilde{C}_J\frac{2tu}{s^2},\\
(t_It_J)_2^{(2)} &= C_IC_J\frac{2su}{t^2} + (\tilde{C}_IC_J + C_I\tilde{C}_J)\frac{st-u^2}{st} + \tilde{C}_I\tilde{C}_J\frac{2tu}{s^2},\\
(t_It_J)_2^{(3)} &= C_IC_J\frac{2su}{t^2} + (\tilde{C}_IC_J + C_I\tilde{C}_J)\frac{tu-s^2}{tu} + \tilde{C}_I\tilde{C}_J\frac{2st}{u^2},
\end{aligned} \tag{16}$$

with a common factor

$$-\left(\frac{\pi}{6}\right)^4 \frac{256g^4}{x^2\bar{x}^2s^2}b^2,$$

(here b is a distance so that $b^2 \geq 0$) and the third one a b^4 hard amplitude, a_4, which is the combination of Eq. (15), but with an overall factor

$$\left(\frac{\pi}{6}\right)^4 \frac{512g^4}{x^2\bar{x}^2s^2}b^4.$$

A check of the above expressions or a possibility to reduce the number of graphs one has to compute is provided by symmetries under meson exchange; starting from the expression one gets with two u-gluon exchange and fermionic flow $f = 1$, see Fig.3, which we label $uu1$, one can generate

Exchange	channel	kinematic	color
$2 \leftrightarrow 4$	$ss1$	$u \leftrightarrow s$	$C \leftrightarrow \tilde{C}$
$3 \leftrightarrow 4$	$tt2$	$u \leftrightarrow t$	$C \leftrightarrow C$
$2 \leftrightarrow 3$	$uu3$	$s \leftrightarrow t$	$C \leftrightarrow \tilde{C}$.

The reader will easily find the channels obtained from another starting point, say $us1$, and the combination of exchanges needed to determine graphs which do not appear in the above array, thus completing the whole amplitude.

4.2 Asymptotic behavior

We are now ready to evaluate the integral defined in Eq. (13) with the above hard amplitudes. In a first step, we approximate the Sudakov factor by its dominant expression at large Q [6]

$$U(x,b,Q) \approx \exp\left[-c\ln\frac{xQ}{\Lambda}(-\ln u(xQ,b) - 1 + u(xQ,b))\right] \exp\left[x \leftrightarrow \bar{x}\right], \tag{17}$$

with

$$u(xQ,b) = \left(-\frac{\ln b\Lambda}{\ln xQ/\Lambda}\right)$$

and $c = 4\,\frac{4}{3}\,\frac{2}{11-2n_f/3} = 32/27$ for $n_f = 3$. We have introduced the variable $u(x,b)$ which turns out to be the relevant one to describe the Sudakov unsuppressed region in the (b,Q)–plane: for $u(xQ,b) = 1$ there is no suppression from the first exponential in Eq. 17; as soon as u departs from unity, one gets rapidly a strong suppression due to the large $\ln xQ$ factor. Eq. (17) is likely to be valid for any Dirac projection because the leading logs factor away independent of spin. In this approximation, U is a scalar in color space and one easily performs the color traces, with

$$c_{I\{a\}}c_{J\{b\}}\prod_{i=1}^{4}\delta_{a_ib_i} = 3\begin{pmatrix} 3 & 1 \\ 1 & 3 \end{pmatrix},$$

$$C_IC_J = \frac{1}{36}\begin{pmatrix} 9 & -3 \\ -3 & 1 \end{pmatrix},\ C_I\tilde{C}_J = \frac{1}{36}\begin{pmatrix} -3 & 9 \\ 1 & -3 \end{pmatrix},$$

$$\tilde{C}_I\tilde{C}_J = \frac{1}{36}\begin{pmatrix} 1 & -3 \\ -3 & 9 \end{pmatrix},$$

and obtains the following hard amplitudes, labeled by the power of b entering:

$$\begin{aligned} a_0 &= \left(\frac{\pi}{6}\right)^4 \frac{256g^4}{x^2\bar{x}^2s^2}\frac{s^4(s^2-3tu)+t^2u^2(s^2-tu)}{s^2t^2u^2}; \\ a_2 &= b^2\left(\frac{\pi}{6}\right)^4 \frac{2048g^4}{x^2\bar{x}^2s^2}\frac{s^4(s^2-3tu)-t^3u^3}{s^2t^2u^2}; \\ a_4 &= b^4\left(\frac{\pi}{6}\right)^4 \frac{2048g^4}{x^2\bar{x}^2s^2}\frac{s^4(s^2-3tu)+t^2u^2(s^2-tu)}{s^2t^2u^2}; \end{aligned} \tag{18}$$

which at 90° is

$$a_0 = 19\left(\frac{\pi}{6}\right)^4 \frac{64g^4}{x^2\bar{x}^2s^2};\ a_2 = 120b^2\left(\frac{\pi}{6}\right)^4 \frac{64g^4}{x^2\bar{x}^2s^2};$$

$$a_4 = 304b^4\left(\frac{\pi}{6}\right)^4 \frac{64g^4}{x^2\bar{x}^2s^2}.$$

For the remaining soft wave function $\mathcal{P}_0$, one can adopt two different models. First, one can approximate $\mathcal{P}_0$ to its value at small b (see [6] and the argument in section 3.1)

$$\mathcal{P}_0(x,b;\mu) \approx \varphi(x;\mu), \tag{19}$$

with

$$\varphi_{\rm as}(x) = 6f_\pi x(1-x), \tag{20}$$

$$\varphi_{\rm cz}(x;\mu\sim 500MeV) = 5(2x-1)^2\varphi_{\rm as}(x), \tag{21}$$

which are standard choices for pion distributions. The asymptotic form Eq. (20) is derived in [1, 7]; it has no evolution with μ and is indeed the limit as $\mu\to\infty$ of all distributions. Because evolution with μ is slow, the effective distribution at non asymptotic regime may

be very different from φ_{as}. Chernyak and Zhitnisky [11] have built from QCD sum rules the above cz-form Eq. (21), which evolves with the scale, but with quite small effects on any computation when one does not examine a huge interval of energy. We will ignore these effects in the following.

The existence of the additional component $\mathcal{P}_1$ complicates the problem. Next to nothing is known about it, but a reasonable ansatz is to adopt a form similar to $\mathcal{P}_0$. One notices that $\mathcal{P}_0$ has a mass dimension which appears to be set by f_π. In the case of $\mathcal{P}_1$, the dimension is a squared mass and we do not know what the normalization constant has to be. We will adjust the normalization in the way described below, and assume the same x–dependence for $\mathcal{P}_0$ as $\mathcal{P}_1$.

For each hard part a_i, freezing the coupling at the scale Q to simplify the study, we get through Eq. (13) a value $A_i(Q, 90^\circ)$ and perform the ratios $R_i = A_i/A_0$.

To get the asymptotic behavior, we analytically evaluate the b-integral

$$\int_0^{\Lambda^{-1}} db\, b^n U(b, x, Q)$$

with a saddle point approximation; using the change of variable $u = -\ln b/\ln\sqrt{x\bar{x}}Q$. One has a maximum of the integrand at $u_0 = \frac{2c}{2c+n+1}$ and finds

$$\int_0^{\Lambda^{-1}} db\, b^n U(b, x, Q) \approx u_0 \sqrt{\frac{\pi \ln Q}{c}} (x\bar{x}Q^2)^{c \ln u_0}. \tag{22}$$

Performing the x-integration

$$I(\varphi, n) = \int_0^1 dx \varphi(x)^4 \left(x(1-x)\right)^{-2+c\ln\frac{2c}{2c+n+1}},$$

an asymptotic expression is found for the ratio

$$R_n(Q) = \frac{2c+1}{2c+n+1} \left(\frac{Q}{\Lambda}\right)^{2c\ln\frac{2c+1}{2c+n+1}} \frac{I(\varphi, n)}{I(\varphi, 0)}, \tag{23}$$

from which one deduces

$$R_2 \propto Q^{-1.10},\ R_4 \propto Q^{-1.85}.$$

Roughly speaking, each power of b is suppressed by $1/\sqrt{Q}$ (not $1/Q$).

4.3 Intermediate behavior

At accessible energies, we expect deviations from the result given in Eq. (23). This comes first from an eventual failure of the saddle point approximation with too small $\ln Q$. We thus have numerically evaluated the amplitude Eq. (13) with U given by Eq. (17). Results for our computation of the ratio of amplitudes are displayed in Fig. 4 with cz distribution (solid line). We get similar results for the asymptotic distribution amplitude (Fig. 5). To fix the normalization, we choose here and in the following to set arbitrarily the ratios to 1 at $\sqrt{s} = 2$GeV. We observe that R_2 decreases by a factor around 7 from $\sqrt{s} = 2$GeV to 20GeV.

This is a much milder suppression than the naively expected $1/Q^2$ factor (dotted curve). R_4 drops more drastically by a factor around 20 in the same energy interval. A numerical study shows that logarithmic corrections ignored within the saddle point approximation are not negligible in the accessible range of energies. At larger values of the energy, $\sqrt{s} > 20\text{GeV}$, the approximated result of Eq. (23) becomes accurate.

Secondly, Eq. (17) should be supplemented with non leading terms which are known in the s-wave case [6] but presumably different in the p-wave case. The neglected logs in the expression of U Eq. (17) may modify soomewhat the ratio over some intermediate range of energy. To modelize such an effect, we add a simple x, b-independent term like

$$\exp\left(K \ln\ln \frac{Q}{\Lambda}\right)$$

in the expression of R_2 with K some constant. The ratio modified by such a factor is shown in Fig. 4 as a shaded area limited by the curves corresponding to $K = 1$ and $K = -1$; this measures in some way the theoretical uncertainty on p-wave contribution suppression. Further theoretical progress in the computation of these $\ln\ln Q$ terms will allow to get rid of this uncertainty but we do not tackle this task here.

A third effect may come from the intrinsic transverse dependence of the wave function. While the replacement of $\mathcal{P}^{(0)}(x, b; 1/b)$ by $\varphi(x; 1/b)$ discussed in section 3.1 is reasonable at large Q ($> 10\text{GeV}$), it is more questionnable at intermediate values where long range physics may be accounted for by including some intrinsic b-dependence [10] as

$$\mathcal{P}_0(x, b) = 4\pi\mathcal{N}\varphi(x) \exp\left(-\frac{\alpha^2}{x\bar{x}} - \frac{x\bar{x}b^2}{4\beta^2}\right). \tag{24}$$

with parameters $\alpha^2 = .096$, $\beta^2 = .88\text{GeV}^2$ and $\mathcal{N} = 1.68$ for the asymptotic distribution amplitude. The results are modified as depicted in Fig. 5 where the curves from this wave function and from the asymptotic distribution are shown for comparison. Furthermore, we notice that the phenomenology may also be modified considerably by allowing variations of different distribution form, that is φ_{as} for $\mathcal{P}_0$ and φ_{cz} for $\mathcal{P}_1$ or the reverse choice.

These three effects show that the power-like decrement Eq. (23) of the ratio is diluted at intermediate energies and consequently the amplitudes A_0 and A_2 are likely to compete over a rather large interval of s, say 1GeV^2–100GeV^2.

5 Helicity violating processes: $\pi\pi \to \rho\rho$ $(h_3 + h_4 \neq 0)$

5.1 Double helicity flip

To begin with, let us find the possible tensorial decomposition for the quark antiquark wave-functions of the ρ meson. One specifies a one particle state by the momentum p_i $(i = 3, 4)$, which with the notation of section 3, one can write: $p_i = Qv_i + \frac{m^2}{2Q}v_i'$ (m is the ρ mass which we do not neglect for the moment), and by the helicity $h_i \in \{1, 0, -1\}$. The 3 helicity states are described in a covariant way with the help of the 3 vectors $\varepsilon_h^\mu(p_i)$, satisfying $\varepsilon_h.p_i = 0$ and

$\varepsilon_h.\varepsilon^*_{h'} = -\delta_{hh'}$. For $\rho(p_3)$, $(\vec{p}_3, \vec{\xi}_3, \vec{\eta})$ is a direct trihedral, and we choose

$$\begin{aligned} (h=+1) \qquad & \varepsilon_R &=& -\frac{1}{\sqrt{2}}(\xi_3 + i\eta), \\ (h=\ \ 0) \qquad & \varepsilon_0 &=& \frac{Q}{m}v_3 - \frac{m}{2Q}v'_3, \\ (h=-1) \qquad & \varepsilon_L &=& \frac{1}{\sqrt{2}}(\xi_3 - i\eta). \end{aligned} \tag{25}$$

A consistent choice for $\rho(p_4)$ is

$$\begin{aligned} (h=+1) \qquad & \varepsilon_R &=& \frac{1}{\sqrt{2}}(\xi_3 - i\eta), \\ (h=\ \ 0) \qquad & \varepsilon_0 &=& \frac{Q}{m}v_4 - \frac{m}{2Q}v'_4, \\ (h=-1) \qquad & \varepsilon_L &=& -\frac{1}{\sqrt{2}}(\xi_3 + i\eta). \end{aligned} \tag{26}$$

Thus, demanding a parity $-$ state, the Bethe-Salpeter amplitude has the most general Dirac-matrices expansion

$$\begin{aligned} &\mathcal{P}(x,b;p,h) = \\ &\mathcal{P}_0\,[\not\varepsilon_h, \not p] + \mathcal{P}'_0\,\not\varepsilon_h + \mathcal{P}_1\,\varepsilon_h.b\,\not p + \mathcal{P}'_1\,\varepsilon_h.b + \tilde{\mathcal{P}}_1\,[\not\varepsilon_h, \not p]\,\not b + \tilde{\mathcal{P}}'_1\,[\not\varepsilon_h, \not b] + \mathcal{P}_2\,\varepsilon_h.b\,[\not p, \not b] + \mathcal{P}'_2\,\varepsilon_h.b\,\not b. \end{aligned} \tag{27}$$

One can then extract the relevant components for the study of independent scattering processes. That is, we isolate dominant high-energy tensors, those which contain one power of the large scale Q and we restrict to b^μ_T (*i.e.* $b\eta^\mu$ in the notation of section 3.1). We get for a longitudinally polarized ρ

$$\mathcal{P}(x, b_T; p, h=0) = \frac{Q}{m}\left(\mathcal{P}'_0\,\not\psi + \tilde{\mathcal{P}}'_1\,[\not\psi, \not b_T]\right), \tag{28}$$

and for a transversally polarized one

$$\mathcal{P}(x, b_T; p, |h|=1) = Q\left(\mathcal{P}_0\,[\not\varepsilon_h, \not\psi] + \mathcal{P}_1\,\varepsilon_h.b_T\,\not\psi + \tilde{\mathcal{P}}_1\,[\not\varepsilon_h, \not\psi]\,\not b_T + \mathcal{P}_2\,\varepsilon_h.b_T\,[\not\psi, \not b_T]\right). \tag{29}$$

Before going through the computation of an helicity violating process, let us exhibit what we call the *double-flip* rule. It follows from the property of each dominant component that each power of b changes the chirality (which is $+$ if the component anticommutes with γ_5 and $-$ if it commutes). With vector gluon couplings, it follows that if the process is allowed by hadron helicity conservation, chiral symmetry requires that the b-components occur in pairs.[2]

[2]The power suppression for amplitudes with extra transverse gluon in initial or final Fock states follows from the same consideration. By power counting one extra gluon embedded into one of the 2 hard scatterings is down by $1/Q$ with respect to the short distance contribution from valence states. However the chirality of the component is the same as the p-wave we are considering (that is opposite to the s-wave). The above argument then applies to ensure that when p-waves and one-gluon components are likely to compete, at least 2 such components are necessary: from section 4, one counts $Q^{-0.55}$ for one p-wave and Q^{-1} for one extra gluon; this shows that considering one extra gluon in the Fock state is indeed subdominant with respect to considering a p-wave state.

We have already encountered this property in the $\pi\pi$ elastic scattering. Furthermore, for an helicity 0-state, in both pseudoscalar and vector case, the chirality of the s-wave term is positive, whereas for an helicity odd state, it is negative. Then with chiral symmetry and because the total power of b has to be even, one concludes that the number of helicity-0 states has to be even too. For a 2 to 2 process, only those processes that violate the helicity conservation rule by two units are expected to be non-zero in the present framework and hence important at large energy.

An example of interaction which satisfies neither the helicity conservation rule nor the double-flip rule is

$$\pi\pi \to \rho_0\rho_T;$$

such an amplitude is thus vanishing by power counting.

We then turn to the study of an helicity violating process which, however, satisfies the double-flip rule, namely $\pi\pi \to \rho_R\rho_R$.

5.2 $\pi\pi \to \rho_R\rho_R$

Let us first verify of the vanishing of the hard amplitude using the s-wave components of the external mesons. For this purpose, it is instructive to examine the connection between quark helicities and the s-wave Dirac tensors we have used until now. This is accomplished in the following way. One considers the free massless spinors of a quark and an antiquark moving in the same direction, the quark having a momentum xp and the antiquark a momentum $\bar{x}p$, so that the compound system has a momentum p. Then one constructs the four possible helicity states of the system with solutions of the Dirac equation and finds

$$\begin{aligned}
(\pi) \qquad & \frac{1}{\sqrt{2}}\left(u_\alpha(xp,\uparrow)\bar{v}_\beta(\bar{x}p,\downarrow) - u_\alpha(xp,\downarrow)\bar{v}_\beta(\bar{x}p,\uparrow)\right) &=& -\sqrt{\frac{x\bar{x}}{2}}\,\gamma_5 \not{p}|_{\alpha\beta} \\
(\rho_0) \qquad & \frac{1}{\sqrt{2}}\left(u_\alpha(xp,\uparrow)\bar{v}_\beta(\bar{x}p,\downarrow) + u_\alpha(xp,\downarrow)\bar{v}_\beta(\bar{x}p,\uparrow)\right) &=& -\sqrt{\frac{x\bar{x}}{2}}\,\not{p}|_{\alpha\beta} \\
(\rho_R) \qquad & u_\alpha(xp,\uparrow)\bar{v}_\beta(\bar{x}p,\uparrow) &=& \sqrt{\frac{x\bar{x}}{2}}\,\not{\epsilon}_R\not{p}|_{\alpha\beta} \\
(\rho_L) \qquad & u_\alpha(xp,\downarrow)\bar{v}_\beta(\bar{x}p,\downarrow) &=& \sqrt{\frac{x\bar{x}}{2}}\,\not{\epsilon}_L\not{p}|_{\alpha\beta}, \qquad (30)
\end{aligned}$$

The helicity conservation rule is then easily verified with these combinations of spinor when one chooses the chiral representation [12]. In this representation, the 2 diagonal blocks of each γ^μ are equal to the null 2×2 matrix. A Feynman-graph fermion line, with vector (or axial) couplings and massless propagator, is an even number of γ–matrices between two spinors:

$$\psi'^\dagger(p',h')\gamma_0\gamma^{\mu_1}\not{k}_1\cdots\not{k}_n\gamma^{\mu_{n+1}}\psi(p,h),$$

Inclusions of γ_5, which is diagonal in this representation, do not modify this property. Then, since to order m/p the chirality of a spinor corresponds to the helicity of the state and, in this representation, chiral eigenstate spinors have either their 2 first components or their two last equal to 0, states of different helicity always give a null product.

This property is algebraic and therefore independent of the representation chosen. However, it is more difficult to observe its effects in the trace formalism described in section 2. Let us examine how it works in the case of the reaction considered. Among the twelve graphs discussed in section 2, each tt and uu graph is 0 because they contain traces over the product of an odd number of γ^μ matrices. For the 8 remaining graphs, the sequence

$$\not\varepsilon_{3R}\not p_3\{\gamma^{\mu_1}\cdots\gamma^{\mu_{2n+1}}\}\not\varepsilon_{4R}\not p_4\cdots$$

occurs (the anticommutation to the left of every γ_5 is understood and does not modify the reasoning). The product of an odd number of γ^μ being a linear combination of γ^μ and $\gamma_5\gamma^\mu$, one is left with the evaluation of

$$\not\varepsilon_R\not p\,\gamma^\mu\not\varepsilon_L\not p'\cdots \quad\text{and}\quad \not\varepsilon_R\not p\,\gamma_5\gamma^\mu\not\varepsilon_L\not p'\cdots,$$

where $v_4 = v_3'$ and $\varepsilon_{4R} = \varepsilon_{3L}$ have been used and the index 3 dropped. One can decompose each γ^μ onto ($\not p$, $\not p'$, $\not\varepsilon_R$, $\not\varepsilon_L$), which are such that their square is 0 and their anticommutation rules are

$$\{\not p,\not\varepsilon_R\} = \{\not p,\not\varepsilon_L\} = \{\not p',\not\varepsilon_R\} = \{\not p',\not\varepsilon_L\} = 0,$$

to conclude that all graphs effectively vanish.

Adding the contribution from one p-wave function does not give any contribution (even before the integration over b), because the total number of γ^μ is necessarily odd. The first non zero term is therefore a b^2 hard amplitude M_2 and the computation, within the approximation of section 4.2, leads to

$$\begin{aligned} M_2\,(\pi\pi\to\rho_R\rho_R) &= \left(\frac{\pi}{6}\right)^4\frac{128g^4}{x^2\bar x^2t^2u^2}b^2\left\{\frac{16(3s^2-7tu)}{3}\mathcal{P}_{1\pi}^2\mathcal{P}_{0\rho}^2-\frac{t^3u^3}{s^4}\mathcal{P}_{0\pi}^2\mathcal{P}_{1\rho}^2\right.\\ &+ 8\frac{t^3u^3}{s^4}\mathcal{P}_{0\pi}^2\mathcal{P}_{0\rho}\mathcal{P}_{2\rho}-16(s^2-3tu)\mathcal{P}_{0\pi}\mathcal{P}_{1\pi}\mathcal{P}_{0\rho}\mathcal{P}_{3\rho}\\ &+ \left.4\frac{t^3u^3}{s^4}\mathcal{P}_{0\pi}^2\mathcal{P}_{1\rho}\mathcal{P}_{3\rho}+4(s^2-3tu+\frac{t^2u^2}{s^2}-2\frac{t^3u^3}{s^4})\mathcal{P}_{0\pi}^2\mathcal{P}_{3\rho}^2\right\}. \end{aligned} \tag{31}$$

This amplitude M_2 has to be supplemented with U (Eq. (17)) and integrated over b and x.

Even though this combination involves several unknown objects, one notices that the angular dependence varies from one component to another and is rather different from the one obtained in $\pi\pi$ elastic scattering. Therefore, it may be possible to analyze the contribution to helicity violation processes from different wave functions and use this information to deduce properties of the wave functions.

The numerical study of section 4 can then be used to understand the energy dependence of double helicity violating processes at accessible energies. As explicitly shown in Fig. 4a and 5, the naive $1/Q^2$ factor is replaced by a milder suppression, and this is primarily due to the specificity of the independent scattering mechanism supplemented by Sudakov effects. Even at very large energies the $Q^{-1.10}$ ratio of Eq. (23) looks quite weak a suppression.

6 Realistic processes and experimental outlook

Studying meson-meson scattering is an unrealistic simplifying assumption. Including baryons is a necessary but quite intricate further step, because of the high number of Feynman diagrams and internal degrees of freedom to be integrated over when more valence quarks are involved. We can however still draw some conclusions from our analysis, leaving to future work a comprehensive study. The mechanism we have explored occurs in several experimentally accessible circumstances. Indeed, there is a host of reactions involving hadronic helicity violation from which we could learn about the interface of perturbative and non-perturbative QCD.

The helicity density matrix of the ρ meson produced in $\pi p \to \rho p$ at 90° is a nice measure of helicity violating components. Experimental data [13] yield $\rho_{1-1} = 0.32 \pm 0.10$, at $s = 20.8\text{GeV}^2$, $\theta_{\text{CM}} = 90^\circ$, for the non-diagonal helicity violating matrix element. Without entering a detailed phenomenological analysis, we may use the results of section 5 through the following line of reasoning. Assuming that the presence of the third valence quark, which is not subject to a third independent scattering, does not alter much the results, one may view ρ_{1-1} as coming from the interference of an helicity conserving amplitude like $\pi\pi \to \rho_L\rho_R$ with a double helicity flip amplitude like $\pi\pi \to \rho_R\rho_R$. We then get a mild energy dependence of this matrix element *i.e.* $Q^{-1.10}$ (Eq. (23)) at asymptotic energies or as shown in Fig. 4a and Fig. 5 at accessible energies. This is at variance with the picture emerging from the diquark model [14]. Measuring the energy dependence of this effect is thus highly interesting.

The most well-known example of hadron helicity violation occurs in $pp \to pp$ scattering [15]. Our demonstration of helicity violating contributions to meson-meson scattering has a bearing on this, because generalized meson scattering is embedded in the diagrams for proton scattering. Without needing to make any dynamical assumption of "diquarks", the perturbative QCD diagrams for $pp \to pp$ scattering contain numerous diquark regions, convolved with scattering of an extra quark. There is no known selection rule which would prevent the scattering of such a subprocess with helicity flip from causing helicity flip in pp elastic scattering. This does not exhaust the possibilities, because there are other channels of momentum flow and color combinatorics which might have different interpretations. The data for $pp \to pp$ also reveals large oscillations about power-law behavior, a second piece of evidence that the short distance picture is inadequate. Elsewhere [16] we have identified these oscillations as a sign of independent scattering. Given the theoretical [17] and experimental evidence, we therefore find no evidence that hadronic helicity conservation is a feature of perturbative QCD, and we believe that independent scattering is a main contender in explaining the observations.

Since reactions of baryons are extremely complicated, and next to nothing is known about the various wave functions in the proton, a productive approach to the question is to ask for experimental circumstances in which the general mechanism we have outlined could be tested without requiring too much detail. We believe that progress here will come from using nuclear targets, and studying the phenomenon of color transparency in hard (as opposed to diffractive) reactions. This program has been outlined elsewhere [18]; it suffices to mention here that suppression of large b^2 regions is expected in reactions of large nuclei. It follows that helicity conservation should be obtained in the same circumstances. Thus the mechanism we have outlined is testable. It is time to go beyond the short-distance physics used to establish

QCD as the correct theory, and we believe that a multitude of phenomena involving spin, color transparency, and detailed hadron structure, will play a major role in the future.

Acknowledgments: This work was supported in part under DOE Grant Number DE FG02 85 ER 40214 and the Kansas Institute for Theoretical and Computational Science, and by the EEC program "Human Capital and Mobility", network "Physics at high energy colliders", contract CHRX–CT93–0357. We thank Stan Brodsky, Steve Heppelmann, Al Mueller, Jacques Soffer, George Sterman, and Joseph Zhitnitsky for useful discussions. Centre de Physique Théorique is *unité propre du CNRS*.

References

[1] S. J. Brodsky and G. P. Lepage, Phys. Rev. D **22**, 2157 (1980).

[2] S.J. Brodsky and G.P. Lepage, Phys. Rev. D **24**, 2848 (1981).

[3] N. Isgur and C. H. Llewellyn Smith, Phys. Rev. Lett. **52**, 1080 (1984), Phys. Lett. **B217**, 535 (1989); A. V. Radyushkin, Nucl. Phys. **A532**, 141 (1991).

[4] P. V. Landshoff, Phys. Rev. D **10**, 1024 (1974).

[5] A. H. Mueller, Phys. Rep. **73**, 237 (1981).

[6] J. Botts and G. Sterman, Nucl. Phys. **B325**, 62 (1989); J. Botts, *ibid.* **B353**, 20 (1991).

[7] G. R. Farrar and D. Jackson, Phys. Rev. Lett. **43**, 246 (1979); S. J. Brodsky and G. P. Lepage, Phys. Lett. **87B**, 359 (1979); A. V. Efremov and A. V. Radyushkin, Phys. Lett. **94B**, 245 (1980); V. L. Chernyak, V. G. Serbo and A. R. Zhitnitsky, Yad. Fiz. **31**, 1069 (1980); A. Duncan and A. H. Mueller, Phys. Rev. D **21**, 1636 (1980). For a recent review, see S. J. Brodsky and G. P. Lepage in *Perturbative QCD*, edited by A. H. Mueller (World Scientific, Singapore, 1989).

[8] J. C. Collins and D. E. Soper, Nucl. Phys. **B193**, 381 (1981) and **B194** (1981) 445.

[9] J.P. Ralston and B. Pire, in *Polarized Collider Workshop* (Penn State University, November 1990) edited by J.C. Collins, *et al.* (AIP Conference Proceedings No. 223) p. 228 and University of Kansas and Ecole Polytechnique preprint A175.0592 (unpublished).

[10] R. Jakob and P. Kroll, Phys. Lett. **315B**, 463 (1993).

[11] V. L. Chernyak and A. R. Zhitnitsky, Phys. Rep. **112**, 173 (1984).

[12] G. R. Farrar and F. Neri, Phys. Lett. **130B**, 109 (1983).

[13] S. Heppelmann *et al.*, Phys. Rev. Lett. **55**, 1824 (1985).

[14] M. Anselmino, P. Kroll and B. Pire, Z. Phys. C **36**, 89 (1987).

[15] P.R. Cameron *et al.*, Phys. Rev. D**32**, 3070 (1985).

[16] B. Pire and J. P. Ralston, Phys. Lett. **117B**, 233 (1982); J. P. Ralston and B. Pire Phys. Rev. Lett. **49** (1982) 1605; *ibid* **61** (1988) 1823; C. E. Carlson, M. Chachkhunashvili and F. Myhrer, Phys. Rev. D **46**, 2891 (1992).

[17] G. R. Farrar, Phys. Rev. Lett. **56**, 1643 (1986); J. P. Ralston and B. Pire, Phys. Rev. Lett. **57**, 2330 (1986).

[18] J. P. Ralston and B. Pire, Phys. Rev. Lett. **65**, 2343 (1990); see also in *Electronuclear Physics with Internal Targets*, edited by R.G. Arnold (World Scientific 1990).

Figure 1: Coordinate space pictures of meson–meson independent scattering. (a) Trajectories of quarks. In the scattering plane quarks approach each other within a distance of order $1/Q$, while the transverse separation of scattering planes (indicated in perspective view) is larger and set by the wave function. (b) Contour map of real part of the product of $m = 0$ leading Sudakov wave functions (from [6]) which give a model for the integrand of Eq. (5). No other soft wave function has been introduced. (c) Same wave function multiplied by a polynomial representing $m = 2$. Contours in (b,c) show flattening in the ξ-direction of the effective wave function imposed by a Gaussian with $b_\xi^2 < 1/Q^2$ at Q^2 =2 GeV^2; higher Q^2 increases the flattening. Units of b_η and b_ξ are fm.

Figure 2: Kinematics of the independent scattering mechanism.

Figure 3: Feynman graphs for the lowest order hard amplitude H; for H' reverse the arrows.

Figure 4: The energy dependence of the R_2 (a) and of the R_4 (b) ratios with cz distribution amplitude [11] (thick lines) and their naive behaviors (thin lines), respectively $1/Q^2$ and $1/Q^4$. The shaded area in (a) indicates uncertainty from neglected logs. The ratios are normalized to 1 at $\sqrt{s}$ =2GeV.

Figure 5: The energy dependence of the R_2 ratio calculated with the asymptotic distribution amplitude with (solid thick line) and without (dashed line) intrinsic b-dependence. The thin line is as in Fig. 4.

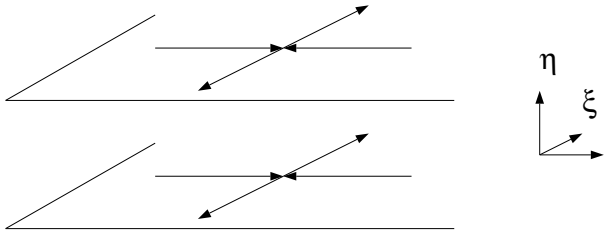

(a)

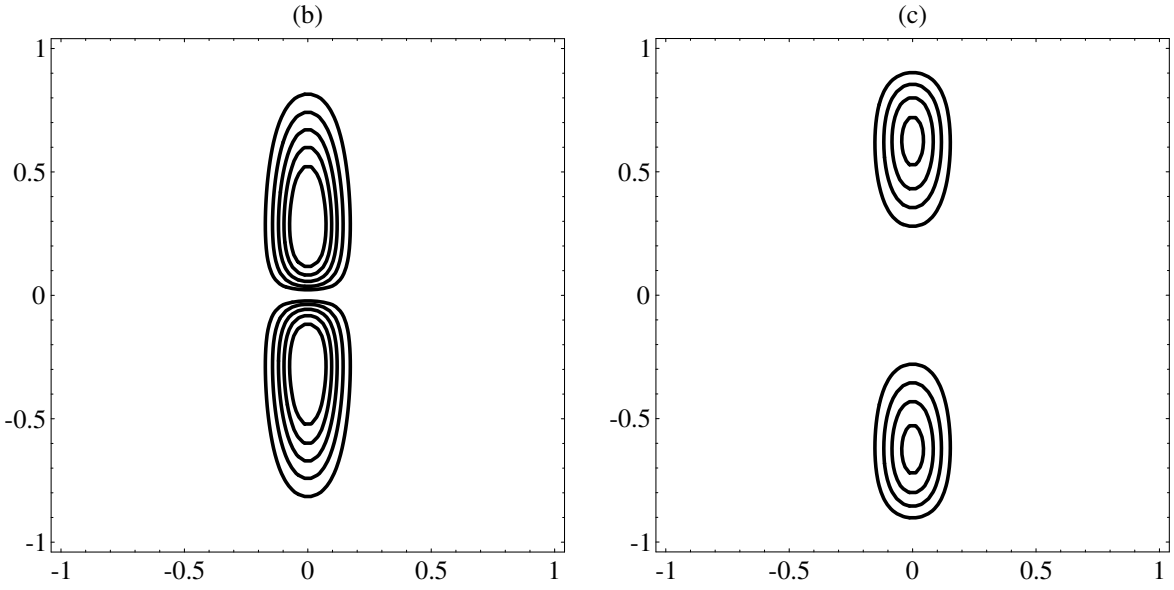

Fig. 1

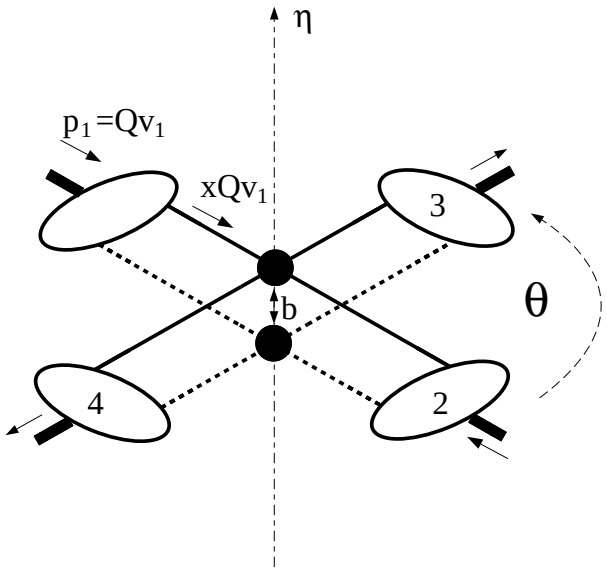

Fig. 2

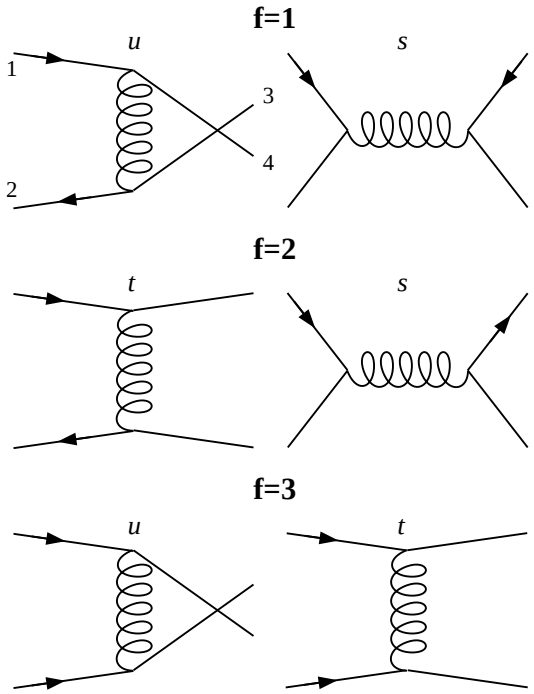

Fig. 3

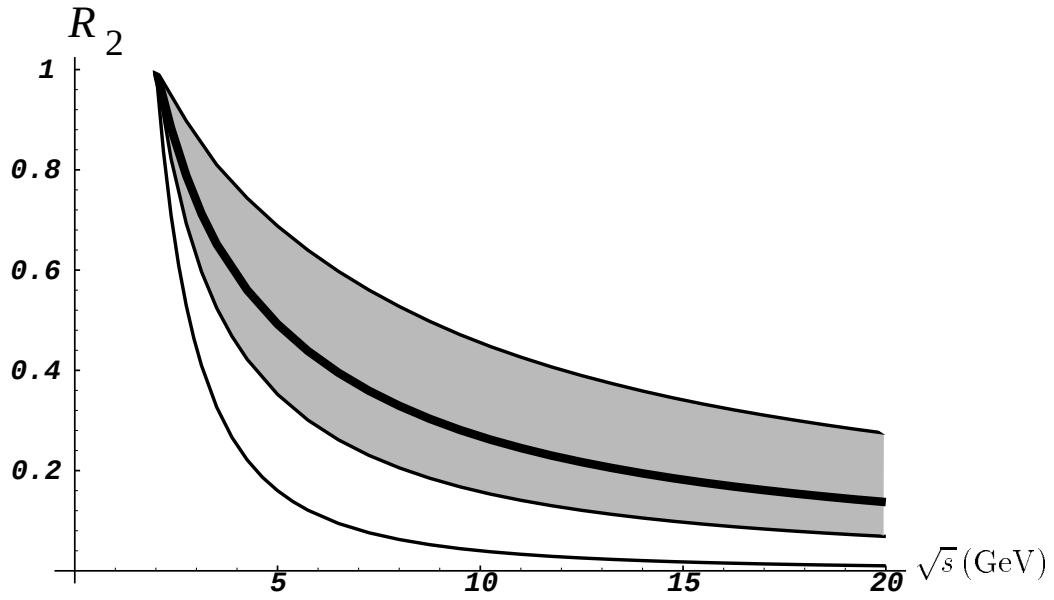

Fig. 4a

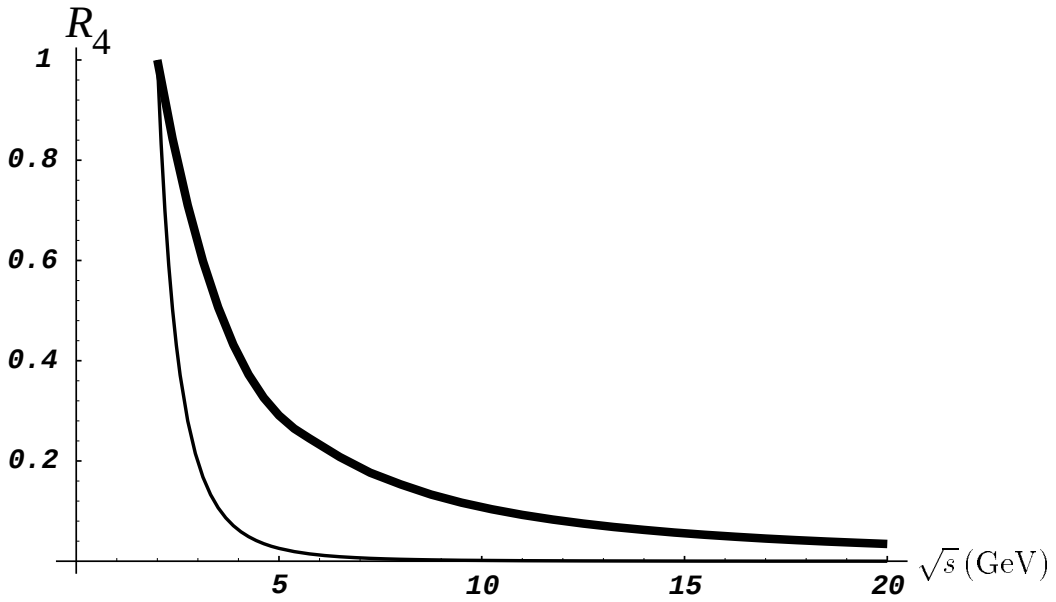
R_4
1
0.8
0.6
0.4
0.2
5
10
15
20
$\sqrt{s}\,(\mathrm{GeV})$

Fig. 4b

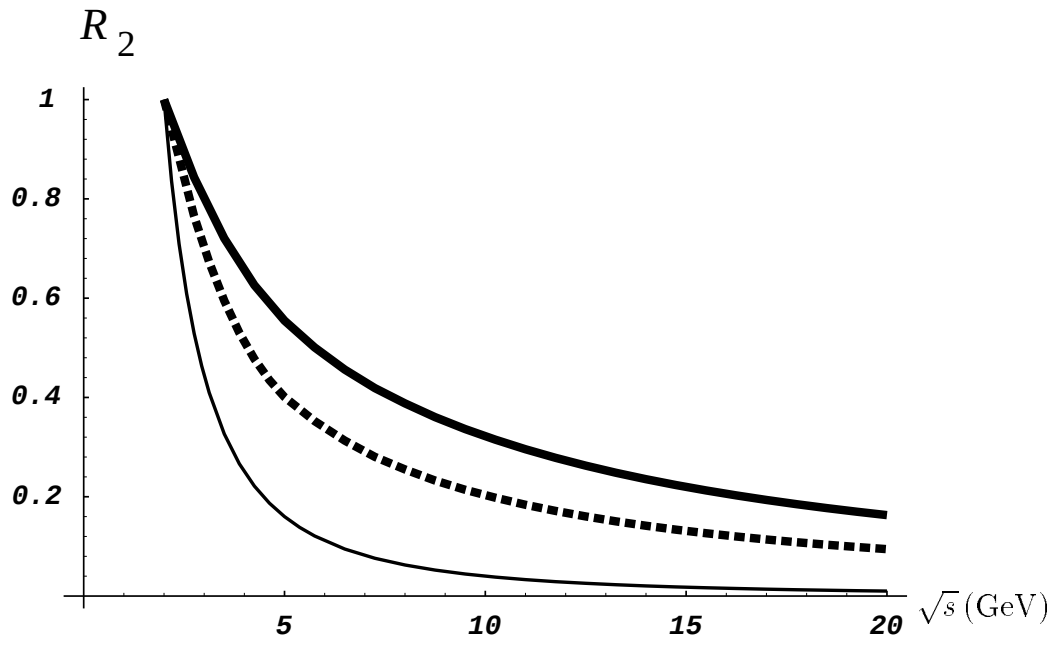
R_2
1
0.8
0.6
0.4
0.2
5
10
15
20
$\sqrt{s}\,(\mathrm{GeV})$

Fig. 5